International Journal of Nanomedicine

Dovepress

open access to scientific and medical research

Open Access Full Text Article

ORIGINAL RESEARCH

Lactoferrin-Bearing Gold Nanocages for Gene Delivery in Prostate Cancer Cells in vitro

Jamal Almowalad[1]
Sukrut Somani[1]
Partha Laskar[1]
Jitkasem Meewan[1]
Rothwelle J Tate[1]
Margaret Mullin[2]
Christine Dufès[1]

[1]Strathclyde Institute of Pharmacy and Biomedical Sciences, University of Strathclyde, Glasgow, G4 0RE, UK; [2]College of Medical, Veterinary and Life Sciences, University of Glasgow, Glasgow, G12 8QQ, UK

Background: Gold nanocages have been widely used as multifunctional platforms for drug and gene delivery, as well as photothermal agents for cancer therapy. However, their potential as gene delivery systems for cancer treatment has been reported in combination with chemotherapeutics and photothermal therapy, but not in isolation so far. The purpose of this work was to investigate whether the conjugation of gold nanocages with the cancer targeting ligand lactoferrin, polyethylene glycol and polyethylenimine could lead to enhanced transfection efficiency on prostate cancer cells in vitro, without assistance of external stimulation.

Methods: Novel lactoferrin-bearing gold nanocages conjugated to polyethylenimine and polyethylene glycol have been synthesized and characterized. Their transfection efficacy and cytotoxicity were assessed on PC-3 prostate cancer cell line following complexation with a plasmid DNA.

Results: Lactoferrin-bearing gold nanocages, alone or conjugated with polyethylenimine and polyethylene glycol, were able to condense DNA at conjugate:DNA weight ratios 5:1 and higher. Among all gold conjugates, the highest gene expression was obtained following treatment with gold complex conjugated with polyethylenimine and lactoferrin, at weight ratio 40:1, which was 1.71-fold higher than with polyethylenimine. This might be due to the increased DNA cellular uptake observed with this conjugate, by up to 8.65-fold in comparison with naked DNA.

Conclusion: Lactoferrin-bearing gold nanocages conjugates are highly promising gene delivery systems to prostate cancer cells.

Keywords: gold nanocages, cancer targeting, transfection efficacy, lactoferrin, polethylenimine, polyethylene glycol

Introduction

Gold nanoparticles have been widely used in biomedical applications due to their low toxicity, tunable size, unique physicochemical properties and ease of surface modification with targeting moieties such as proteins, peptides and antibodies to specifically target cancer cells.[1–3] In addition to these properties, they have been particularly attractive for gene delivery, owing to their ability to condense nucleic acids via electrostatic interactions or through the conjugation of nucleic acids to their surface via thiol linkages.[4–7] Among these nanoparticles, gold nanocages are a novel class of gold nanomaterial with cage shape, hollow interiors and porous wall that allow them to load drugs, in addition to their ability to convert light into heat at near-infrared region (700–900 nm), making them appropriate candidates for biomedical applications and photothermal cancer therapy.[8–10] Due to the unique

Correspondence: Christine Dufès
Strathclyde Institute of Pharmacy and Biomedical Sciences, University of Strathclyde, Glasgow, G4 0RE, UK
Tel +44 1415483796
Fax +44 1415522562
Email C.Dufes@strath.ac.uk

Graphical Abstract

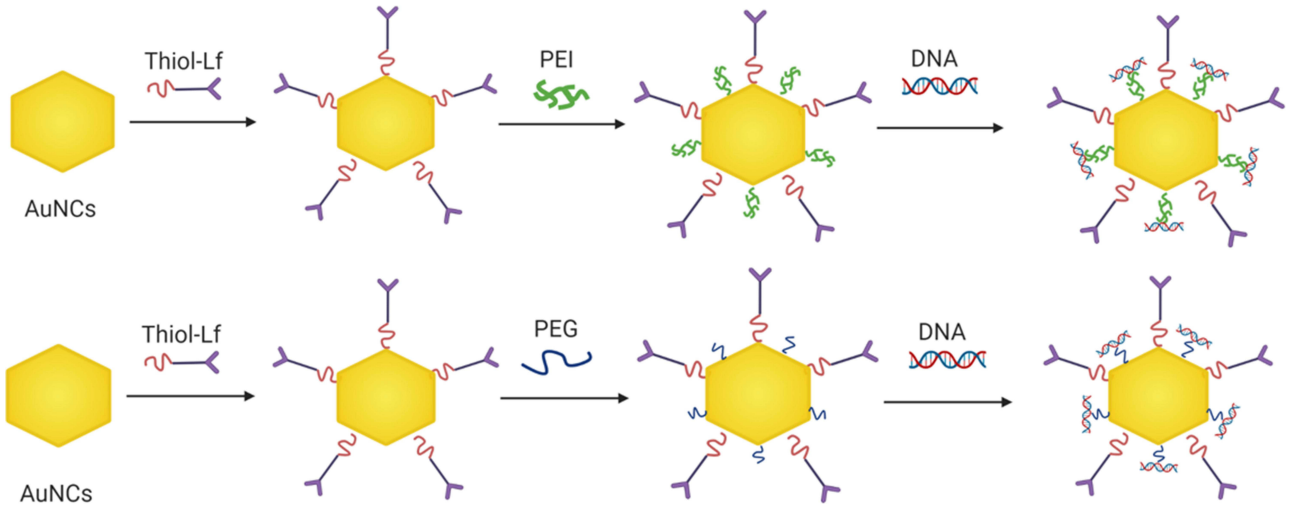

structure of gold nanocages, drugs can be loaded into the hollow interiors of the nanocages that are then coated by a shell of thermo-sensitive polymers, as previously reported.[11,12] The polymer shell prevented the drug from being released until external thermal stimuli such as near-infrared light or high-intensity-focused ultrasound were presented.

However, the recent advances of the use of gold nanocages in controlled drug delivery and photothermal cancer therapy led to the need to explore the possibility of using gold nanocages for targeted gene delivery for cancer treatment, without the assistance of external stimulations or combination with chemotherapeutics. Hence, we propose to conjugate the surface of gold nanocages with cancer-targeting moieties such as lactoferrin and to functionalize the nanocages surface with cationic polymers, and investigate whether the conjugated gold nanocages could condense the DNA on their surface and facilitate gene expression on prostate cancer cells in vitro. Recently, cancer-targeting ligand lactoferrin (Lf), whose receptors are overexpressed in most cancers, has been shown to be highly promising in enhancing the therapeutic efficacy of gene cancer therapy as a result of significant increase of gene expression in tumors after intravenous administration.[13–15] Cationic polymers, such as polyethylenimine (PEI), have been widely used to generate positively charged nanoparticles due to its capacity to complex DNA or RNA and to its high transfection efficiency.[7,16] Furthermore, low molecular weight PEI resulted in decreased cytotoxicity and enhanced transfection efficacy compared to its high molecular weight counterpart.[17] The conjugation of polyethylene glycol (PEG) to nanoparticles is another approach that has recently contributed to enhance transfection efficiency while reducing the cytotoxicity associated with nanoparticles through shielding their charges and preventing their interactions with plasma proteins.[18–20]

The objectives of this study were therefore to (1) synthesize and characterize lactoferrin-bearing gold nanocages, PEG-conjugated, lactoferrin-bearing gold nanocages and PEI-conjugated, lactoferrin-bearing gold nanocages, (2) to evaluate their DNA condensation efficiency following complexation with a plasmid DNA, and (3) to assess the cell viability, transfection efficacy and cellular uptake of these conjugates complexed with DNA on PC-3 prostate cancer cells.

Materials and Methods

Cell Lines and Reagents

Lactoferrin (Lf), branched polyethyleneimine (PEI, Mw 800 Da), diethylene glycol (DEG), silver trifluoroacetate (CF_3COOAg), sodium hydrosulfide hydrate (NaSH), hydrogen tetrachloroaurate (III) hydrate ($HAuCl_4$), aqueous hydrochloric acid solution (HCl, 37%), polyvinyl pyrrolidone (PVP, Mw 55,000 Da), sodium chloride (NaCl) and deionized (DI) water with a resistivity of 18.2 MΩ·cm were purchased from Sigma Aldrich (Poole, UK). Thiol PEG amine (HS-PEG3.5K-NH_2) was from

JenKem Technology (Plano, TX). N-[1-(2,3-Dioleoyloxy) propyl]-N,N,N-trimethylammonium methylsulfate (DOTAP) liposomal transfection reagent was purchased from Roche (Burgess Hill, UK). The expression plasmid encoding β-galactosidase (pCMVsport β-galactosidase) was obtained from Invitrogen (Paisley, UK). It was purified using an Endotoxin-free Giga Plasmid Kit (Qiagen, Hilden, Germany). Minimum Modified Eagle Medium (MEM) and fetal bovine serum (FBS), L-glutamine and penicillin-streptomycin were obtained from Life Technologies (Paisley, UK). Vectashield® mounting medium containing 4′,6-diamidino-2-phenylindole (DAPI) was ordered from Vector Laboratories (Peterborough, UK). Label IT® Fluorescein Nucleic Acid Labeling Kit was obtained from Cambridge Biosciences (Cambridge, UK). Passive lysis buffer was purchased from Promega (Southampton, UK). BioWare® androgen-irresponsive PC-3M-luc-C6 human prostate adenocarcinoma that expresses the firefly luciferase was purchased from Caliper Life Sciences (Hopkinton, MA).

Synthesis and Characterization of Gold Nanocages Conjugates

Synthesis of Silver Nanocubes

Silver nanocubes were synthesized via polyol reduction in diethylene glycol (DEG) as previously reported.[21] Briefly, 60 mL of DEG was added into 250 mL round-bottom flask containing a magnetic stir bar and heated in an oil bath at 150 °C for 30 min. The reagents were then prepared in DEG and added separately to the reaction flask. Initially, NaSH solution (0.72 mL, 3 mM) was pipetted to the flask. After 4 min, HCL solution (6 mL, 3 mM) was added, followed by 15 mL of PVP solution (20 mg/mL). After 2 min, CF_3COOAg solution (4.8 mL, 282 mM) was then added. The flask was closed loosely throughout the entire process, except during the addition of the reagents. The reaction was stopped after 90 min by placing the flask in an ice water bath for 30 min. Then, 25 mL of the mixture was transferred to 50 mL centrifuge tube and mixed with 20 mL acetone, followed by centrifugation at 9000 rpm (16,000 g) for 30 min. After removing the supernatant, 20 mL of deionized (DI) water was added to the remaining products then sonicated for 10 min using an ultrasound bath sonicator. Next, the products were centrifuged at 9000 rpm (16,000 g) for 10 min, followed by the discarding of the supernatant and the sonication of the remaining products with 20 mL of DI water. This process was repeated a further three times. The final products were then dispersed in 20 mL of DI water and stored at 4 °C.

Synthesis of Gold Nanocages

Gold nanocages (AuNCs) were synthesized based on previously published methods,[22] with some modifications. Briefly, 600 mL of polyvinyl pyrrolidone (PVP) solution (1 mg/mL in DI water) was added to a 1 L round-bottom flask containing a magnetic stir bar. Then, 60 mL of as-prepared silver nanocubes were added to the flask and heated at 100 °C, while stirring for 30 min. An aqueous solution of 1 mM $HAuCl_4$ (140 mL) was added to the reaction flask via a syringe pump at a rate of 45 mL/h. The reaction was stopped when the reaction sample attained a blue color and exhibited UV-Vis absorption spectrum at 740 nm. The mixture was heated at 100 °C for another 15 min until the reaction color became stable. After cooling down the flask to 25 °C, 20 mL of NaCl-saturated solution (0.36 g/mL) was mixed with each 25 mL aliquots of the mixture to remove AgCl. The products were then centrifuged at 9000 rpm (16,000 g) for 30 min and washed with 20 mL of DI water after discarding the supernatant. This process was repeated three times. The final products were added to 20 mL of DI water and stored at 4 °C for further use. Au concentration of gold nanocages was obtained via inductively coupled plasma mass spectrometry (ICP-MS). Briefly, 20 µL of AuNCs in DI water was digested in 180 µL aqua regia at 20 °C for 1 h. The mixture was further diluted with DI water to a final aqua regia concentration of 2%. The Au concentration (µg/L) within the samples was measured using the ^{197}Au isotope and the ^{175}Lu isotope used as an internal standard for all measurements. All ICP-MS measurements were performed in triplicate using an Agilent 7700X® instrument (Agilent Technologies, Santa Clara, US).

Synthesis of Lactoferrin-Bearing Gold Nanocages (AuNCs-Lf)

The conjugation of lactoferrin (Lf) to AuNCs was done with modifications from a previously reported method.[23] Briefly, 8 mg of Lf was dissolved in 2 mL of 50 mM sodium phosphate and 0.15 M sodium chloride buffer (pH 7.5) and reacted with 5-fold mole excess of 2-iminothiolane (Traut's reagent, 1 mg/mL in distilled water, 7.26 mM, 61.2 µL) for 75 min at 20 °C. The modified Lf was purified using a Vivaspin-6 centrifuge tube with a molecular weight cut-off (MWCO) of 5000 Da for 20

min at 8000 rpm (14,000 g). Thiolated Lf (100 µL, 8 mg/mL) was added to 1 mL of AuNCs, then vortexed and incubated at 25 °C for 24 h. The final product was purified twice with 1 mL of DI water using Vivaspin-6 centrifuge tubes with a MWCO of 100,000 Da to remove any unreacted AuNCs, before being freeze-dried.

Synthesis of PEG-Conjugated, Lactoferrin-Bearing Gold Nanocages (AuNCs-Lf-PEG)

Thiol-PEG3.5K-amine aqueous solution (100 µL, 2 mM) was added to 1 mL of lactoferrin-bearing AuNCs (AuNCs-Lf) suspension and vortexed for 10 s. The mixture was then incubated at 25 °C for 24 h. The final product was purified twice with DI water using Vivaspin-6 centrifuge tubes with MWCO of 100,000 Da to remove any unreacted PEG, before being freeze-dried.

Synthesis of PEI-Conjugated, Lactoferrin-Bearing Gold Nanocages (AuNCs-Lf-PEI)

The thiolation of polyethyleneimine (PEI) was performed with modifications of a previously reported method.[24] The formation of thiolated PEI was carried out by reacting the PEI with 2-fold moles excess of 2-iminothiolane (Traut's reagent). PEI was dissolved in PBS at a concentration of 10 mg/mL (12.5 mM). Traut's reagent (3.44 mg/mL in PBS, 25 mM, 4.28 mL) was added to PEI solution (10 mg/mL in PBS, 12.5 mM, 4.28 mL) and vortexed for 5 s. The reaction mixture was then incubated at 25 °C for 24 h. The final compound was purified using benzoylated dialysis tubing with a MWCO of 2000 Da at room temperature (20–22 °C) against 2 L of distilled water and changed twice during dialysis. After 24-hour dialysis, the solution was freeze-dried for 48 hours using Christ Epsilon 2–4 LSC® freeze dryer (Osterode am Harz, Germany).

Thiolated PEI (10 mg/mL in PBS, 400 µL) was added to each 1 mL of as-prepared AuNCs-Lf, vortexed for 5 s, then incubated at 25 °C for 24 h. AuNCs-Lf-PEI was then purified twice with 1 mL of DI water using a Vivaspin-6 centrifuge tube with a MWCO of 5000 Da for 20 min at 8000 rpm (14,000 g). The purified AuNCs-Lf-PEI conjugate was freeze-dried for 48 hours.

Characterization of Gold Nanocages Conjugates

Transmission Electron Microscopy

The morphology of AuNCs conjugates was examined using transmission electron microscopy (TEM). Typically, 20 of µL AuNCs conjugates samples were placed in carbon-coated 200-mesh copper grids and left to dry at 20 °C for 1 h. The samples were then visualized using a JEOL JEM-1200EX® transmission electron microscope (Jeol, Tokyo, Japan) operating at an accelerating voltage of 80 kV.

Circular Dichroism Spectrometer

The conjugation of Lf, Lf-PEG and Lf-PEI to AuNCs was assessed using circular dichroism (CD) spectrometer (Chirascan V100®, Applied Photophysics, Leatherhead, UK). All samples were prepared at a concentration of 2 mg/mL in DI water. CD spectra were recorded using a quartz cuvette with a path length of 10 mm over a range of 190–900 nm, with a scan speed of 70 nm/min and a bandwidth of 1 nm.

Fourier-Transform Infrared Spectrophotometer (FTIR)

The infrared spectra of Lf-bearing AuNCs were carried out using Fourier-transform infrared (FTIR) spectrophotometer equipped with attenuated total reflectance (ATR) probe (IRSpirit® QATR-S, Shimadzu, Kyoto, Japan). Transmission spectra were collected over a range of 4000–400 cm^{-1} at a resolution of 4 cm^{-1}, then analyzed with the LabSolutions IR® software (Shimadzu, Kyoto, Japan).

UV-Vis Spectrometry Analysis

The formation of the AuNCs conjugates was further evaluated by UV-Vis spectrometry analysis using a Varian Cary® 50 Bio UV-visible spectrophotometer in the wavelength range of 300–900 nm. The UV-Vis spectrum of DI water was adjusted as baseline prior to the measurement of the samples.

Size and Zeta Potential Measurement

The size and zeta potential of AuNCs conjugates in DI water were measured by photon correlation spectroscopy and laser Doppler electrophoresis using a Malvern Zetasizer Nano-ZS® (Malvern Instruments, Malvern, UK) at 25 °C. All size and zeta-potential measurements were conducted in triplicate with a He–Ne laser operating at 632.8 nm and a scattering angle of 173°.

Characterization of the Complexation of AuNCs-Lf, AuNCs-Lf-PEG and AuNCs-Lf-PEI Conjugates with DNA

Gel Retardation Assay

The ability of AuNCs conjugates to condense DNA was assessed by agarose gel retardation assay. AuNCs

conjugate complexes were prepared at various AuNCs conjugate:DNA weight ratios from 0.5:1 to 40:1, with a constant DNA concentration of 20 µg/mL. After mixing with the loading buffer, the samples (15 µL) were loaded on a 1X Tris-Borate-EDTA (TBE) (89 mM Tris base, 89 mM boric acid, 2 mM Na_2-EDTA, pH 8.3) buffered 0.8% (w/v) agarose gel containing ethidium bromide (0.4 µg/mL), with 1x TBE as a running buffer. The DNA size marker was HyperLadder I. The gel was run at 50 V for 1h and then photographed under UV light.

Size and Zeta Potential of the Complexes

The size and zeta potential of the complexes in 5% (w/v) glucose were measured for different AuNCs conjugates: DNA weight ratios (0.5:1, 1:1, 5:1, 10:1, 20:1, 40:1) by photon correlation spectroscopy and laser Doppler electrophoresis at 37 °C using a Malvern Zetasizer Nano-ZS® (Malvern Instruments, Malvern, UK). The DNA concentration (1 µg/mL) remained constant throughout the experiment.

Cell Culture

PC-3-Luc prostate cancer cells were grown as monolayers in Minimum Essential Medium (MEM) supplemented with 10% (v/v) fetal bovine serum, 1% (v/v) L-glutamine, and 0.5% (v/v) penicillin–streptomycin. The cell culture flasks were kept at 37 °C in a 5% carbon dioxide humid atmosphere.

Transfection

The transfection efficacy of the DNA complexed to AuNCs conjugates was assessed using a β-galactosidase assay. PC-3 cells were seeded at a concentration of 10,000 cells/well in 96-well plates and incubated for 24 h at 37 °C in a 5% CO_2 atmosphere. They were then treated with AuNCs conjugates complexed with a plasmid DNA encoding β-galactosidase, in quintuplicate at various AuNCs conjugate:DNA weight ratios (0.5:1, 1:1, 2:1, 5:1, 10:1 20:1 and 40:1). Naked DNA was used as a negative control, whereas DOTAP-DNA (weight ratio 5:1) served as a positive control. DNA concentration (0.5 µg/well) was maintained constant throughout the experiment. The cells were incubated for 72 h with the treatment before analysis. They were then lysed with 1x passive lysis buffer (PLB) (50 µL/well) for 20 min and then tested for β-galactosidase expression.[25] Briefly, 50 µL of the assay buffer (2 mM magnesium chloride, 100 mM mercaptoethanol, 1.33 mg/mL o-nitrophenyl- β-D-galactosidase, 200 mM sodium phosphate buffer, pH 7.3) was added to each well containing the lysate, before being incubated for 2 h at 37 °C. The absorbance of the samples was subsequently read at 405 nm using a Multiskan Ascent® plate reader (MTX Lab Systems, Bradenton, FL).

Cellular Uptake

Quantitative Analysis

The quantification of cellular uptake of DNA complexed with AuNCs conjugates was carried out by flow cytometry. PC-3 cells were seeded at a density of 3×10^5 cells per well in 6-well plates and grown at 37 °C for 24 h, before being treated with fluorescein-labeled DNA (2.5 µg DNA per well) alone or complexed with the conjugates at AuNCs conjugate:DNA weight ratios of 0.5:1 and 40:1. Untreated cells served as a negative control. After 24 h of incubation with the treatments, each well was washed with 2 mL of PBS pH 7.4 twice. Single-cell suspensions were then prepared (using 250 µL trypsin per well, followed by 500 µL medium per well once the cells were detached), before being analyzed using a FACSCanto® flow cytometer (BD, Franklin Lakes, NJ). Their mean fluorescence intensity was analyzed with FACSDiva® software (BD, Franklin Lakes, NJ), counting 10,000 cells (gated events) for each sample.

Qualitative Analysis

The cellular uptake of DNA complexed with AuNCs conjugates was qualitatively assessed using confocal microscopy. The labeling of plasmid DNA with the fluorescent probe fluorescein was performed using a Label IT® Fluorescein Nucleic Acid Labeling kit, as described by the manufacturer. PC-3 cells were seeded on coverslips in 6-well plates at a concentration of 3×10^5 cells per well and grown for 24 h at 37 °C. The cells were then treated with fluorescein-labeled DNA (2.5 µg /well) complexed to AuNCs-Lf-PEI at weight ratio of 40:1 for 24 h at 37 °C. Control wells were also prepared with naked DNA or were left untreated. The cells were then washed twice with 3 mL PBS before being fixed with 2 mL methanol for 10 min at 20 °C. They were then washed again once with 3 mL PBS. Upon staining of the nuclei with Vectashield® mounting medium containing DAPI, the cells were examined using a Leica TCS SP5® confocal microscope (Wetzlar, Germany). DAPI (which stained the cell nuclei) was excited with a 405 nm laser line (emission bandwidth: 415–491 nm), and fluorescein (which labeled the DNA)

was excited with a 514 nm laser line (emission bandwidth: 550–620 nm).

Cell Viability

The viability of PC-3 prostate cancer cells treated with the AuNCs conjugates was assessed using a standard MTT assay. PC-3 cells were seeded in quintuplicate at a density of 10,000 cells/well in 96-well plates and incubated at 37 °C for 24 h. The cells were then treated with various concentrations of AuNCs conjugates ranging from 2.5 to 200 µg/mL for 72 h at 37 °C and 5% CO_2. Following incubation with the treatment, 50 µL of the MTT solution (5 mg/mL in PBS pH 7.4) was added to the medium and incubated at 37 °C, protected from light for four hours. The medium was then replaced with 200 µL of DMSO per well to dissolve the precipitated formazan. The absorbance was measured at 570 nm using a Multiskan Ascent® plate reader (Thermo Scientific, Waltham, MA).

Statistical Analysis

Results were expressed as means ± standard error of the mean (SEM). Statistical significance of the data was assessed by one-way analysis of variance (ANOVA) and Tukey multiple comparison post-test (Minitab® 17.1.0 software, State College, PE). Differences were considered statistically significant for P values lower than 0.05.

Results

Characterization of AuNCs Conjugates

Gold nanocages were synthesized via a galvanic replacement reaction between Ag nanocubes and chloroauric acid ($HAuCl_4$). Their large volume batch (800 mL) with Au content of 597.93 µg/L was used for all the experiments described in this manuscript.

TEM images confirmed the cage-shape, hollow interior and thin wall of the gold nanocages, with an edge length of 50 nm (Figure 1).

The conjugation of Lf to the surface of AuNCs was demonstrated using CD and FTIR spectroscopy. The CD spectrum of Lf exhibited distinctive negative ellipticity peaks at 244 nm and 283 nm, and a positive ellipticity peak at 309 nm (Figure 2). These peaks were visible in the CD spectrum of AuNCs-Lf, unlike that of unmodified AuNCs, indicating that Lf was successfully conjugated to the surface of AuNCs. The highest molar ellipticity values for the Lf protein and the conjugates at identical wavelengths (244 nm and 283 nm) indicated that there was no significant conformational change in the protein folding upon grafting to the nanocages.

FTIR spectrum of AuNCs-Lf showed the presence of characteristics peaks at 1645.01 cm^{-1} and 1534.86 cm^{-1} (corresponding to amide-I and amide-II of bare Lf) and the absence of peaks at 1049.94 cm^{-1} and 1398.97 cm^{-1} (respectively corresponding to the sulfoxide and sulfate groups of thiolated lactoferrin), in comparison with the starting materials (Figure 3). These findings therefore confirmed the successful conjugation of Lf to the surface of gold nanocages via Au-S bond and demonstrated the absence of significant changes on the protein secondary structure, consistently with the data obtained from CD.

The conjugation of Lf, PEG and PEI to the surface of AuNCs was further confirmed by UV-Vis spectrometry analysis. AuNCs and AuNCs conjugates exhibited UV-Vis spectra peaks in the near-infrared region (715 nm, 771 nm, 767 nm and 813 nm respectively for AuNCs, AuNCs-Lf, AuNCs-Lf-PEG and AuNCs-Lf-PEI) (Figure 4). The red-shift of the UV-Vis spectra of AuNCs-Lf, AuNCs-Lf-PEG and AuNCs-Lf-PEI compared to AuNCs confirmed the

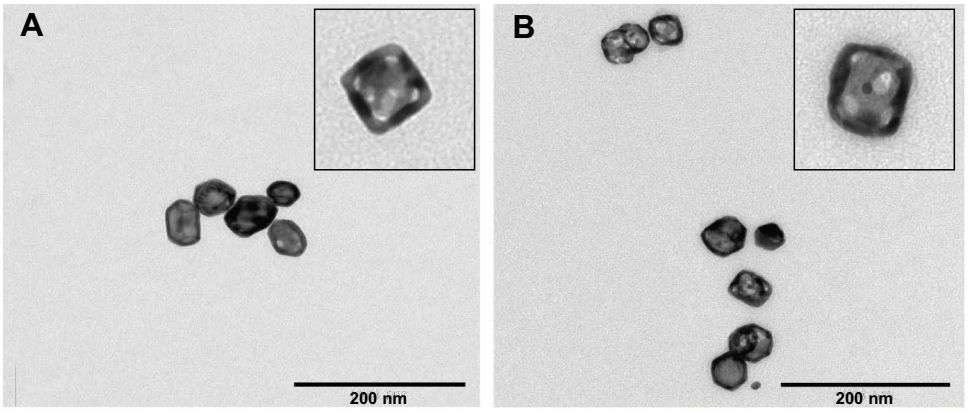

Figure 1 Transmission electron microscopic images of gold nanocages (**A**) and lactoferrin-bearing gold nanocages (**B**). Insets: magnification of the samples showing the morphology of the nanocages.

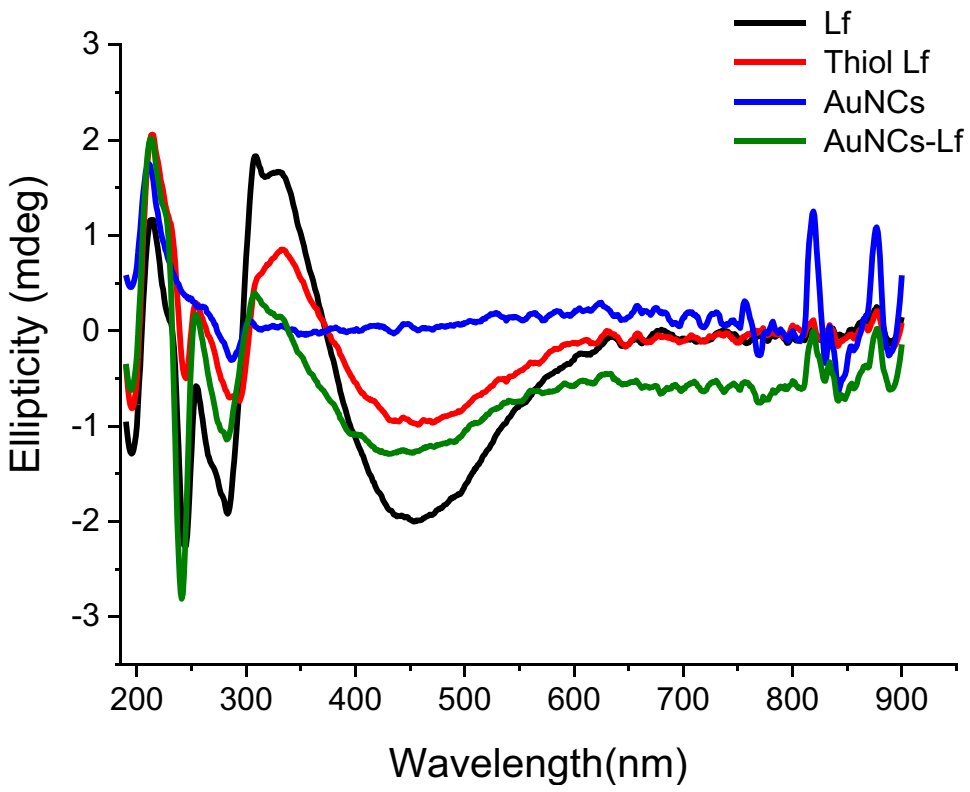

Figure 2 CD spectra of lactoferrin ("Lf"), thiolated lactoferrin ("Thiol Lf"), unmodified gold nanocages ("AuNCs") and lactoferrin-bearing gold nanocages ("AuNCs-Lf").

surface modification of AuNCs with Lf and indicated an efficient conjugation of PEG and PEI to AuNCs-Lf.

The conjugation of Lf, Lf-PEG and Lf-PEI to the surface of the AuNCs resulted in a slight increase in the hydrodynamic size of AuNCs-Lf (105.40 ± 0.43 nm), AuNCs-Lf-PEG (103.30 ± 1.31 nm) and AuNCs-Lf-PEI (127 ± 1.62 nm) compared to that of AuNCs (88.69 ± 0.66 nm), as determined by DLS measurements. It also increased the net surface charge of the gold nanocages, from negative (−20.50 ± 0.38 mV) in the case of unmodified AuNCs, to positive (3.05 ± 0.18 mV, 4.11± 0.38 mV and 14.10 ± 0.14 mV) for AuNCs-Lf, AuNCs-Lf-PEG and AuNCs-Lf-PEI, respectively.

Characterization of AuNCs-Lf-DNA Complex Formation

Gel Retardation Assay

A gel retardation assay confirmed the complete or partial DNA condensation by AuNCs-Lf and AuNCs-Lf-PEG. At a AuNCs conjugate:DNA weight ratio of 40:1, DNA was fully condensed by AuNCs-Lf and AuNCs-Lf-PEG, thus preventing ethidium bromide to intercalate with DNA. No free DNA was therefore visible at this ratio (Figure 5A and B). In contrast, DNA was partially condensed by AuNCs-Lf and AuNCs-Lf-PEG at ratios 20:1 and lower. Ethidium bromide could therefore intercalate with DNA and a band corresponding to free DNA was visible. On the other hand, AuNCs-Lf-PEI was able to completely condense DNA at weight ratios higher than 1:1, resulting in the absence of a band corresponding to free DNA at these ratios (Figure 5C). Among the 3 AuNCs conjugates assessed in this study, AuNCs-Lf-PEI was therefore the most efficacious in condensing DNA at conjugate:DNA weight ratios higher than 1:1.

Size and Zeta Potential of the Complexes

AuNCs conjugates complexed with DNA displayed an average hydrodynamic size smaller than 250 nm at conjugate:DNA weight ratios higher than 1:1 for AuNCs-Lf and AuNCs-Lf-PEG, and higher than 5:1 for AuNCs-Lf-PEI (Figure 6A). The average size of complexes decreased with increasing weight ratios, from 0.5:1 to 5:1, then reached a plateau from a 10:1 weight ratio. Among AuNCs conjugate complexes, AuNCs-Lf-PEI exhibited the largest complex size of 1.50 ± 0.02 μm at a weight ratio 0.5:1, while AuNCs-Lf and AuNCs-Lf-PEG complexes had smaller size diameter of 464.00 ± 37.37 nm

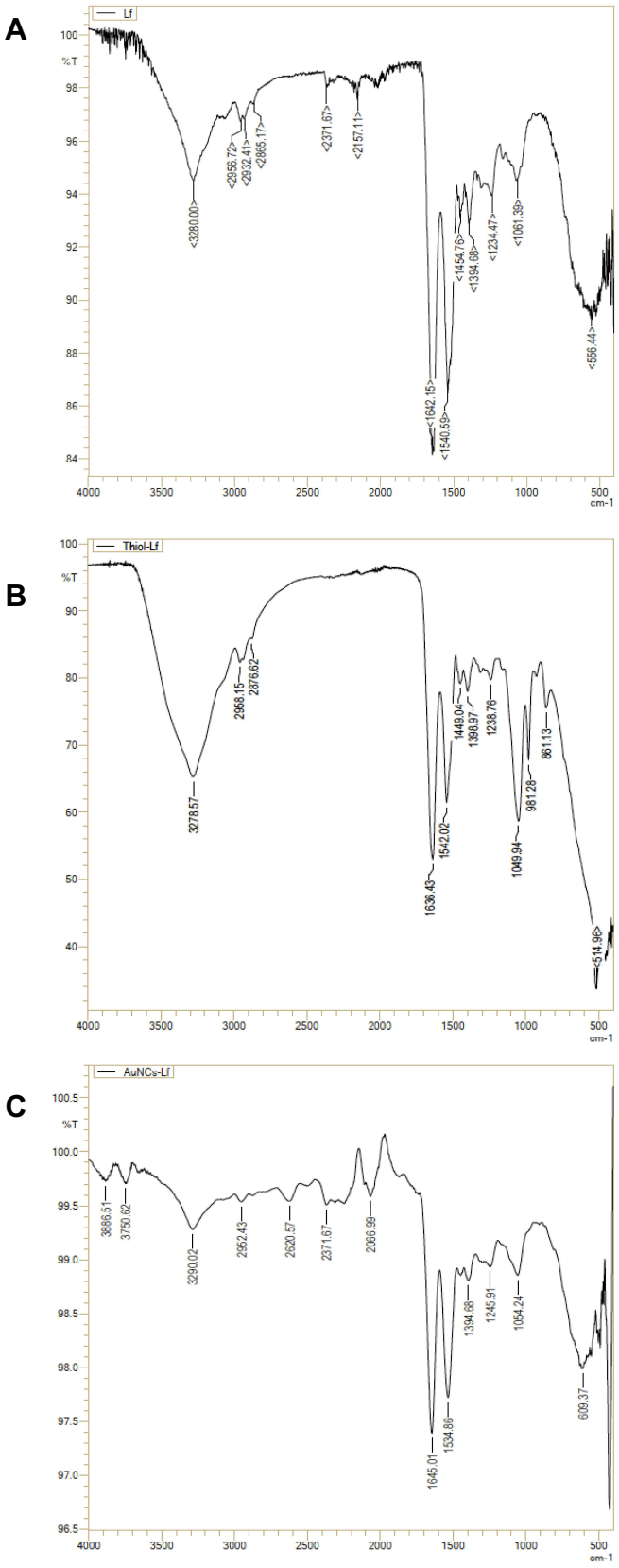

Figure 3 FTIR spectra of (**A**) lactoferrin ("Lf"), (**B**) thiolated lactoferrin ("Thiol Lf") and (**C**) lactoferrin-bearing gold nanocages ("AuNCs-Lf").

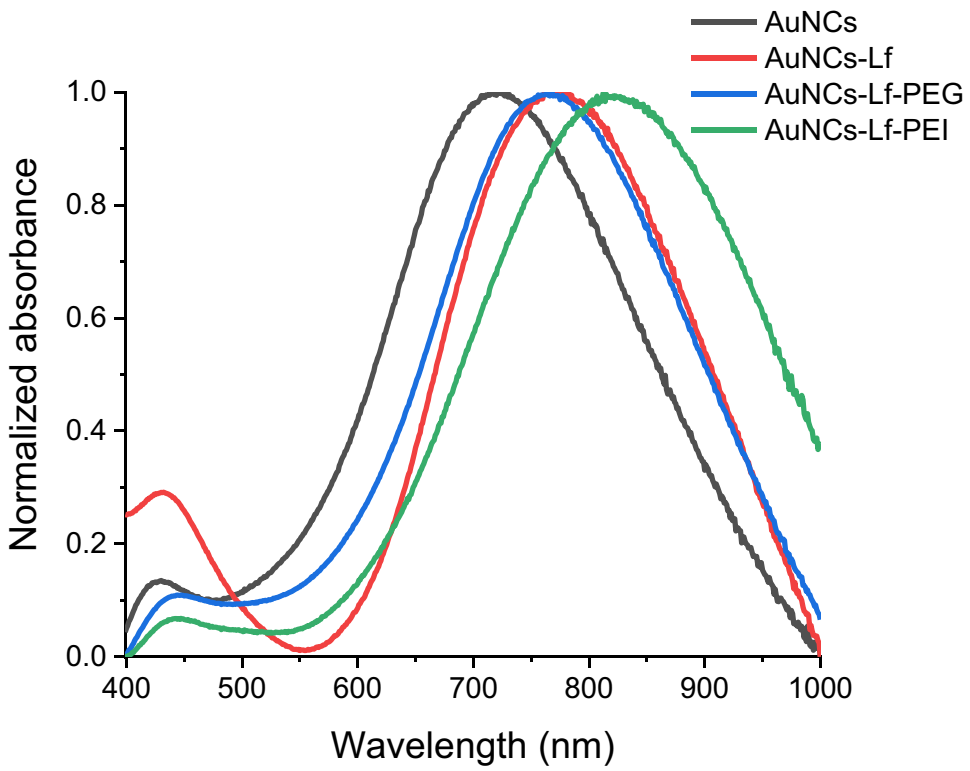

Figure 4 UV-Vis spectra of AuNCs, AuNCs-Lf, AuNCs-Lf-PEG, AuNCs-Lf-PEI conjugates.

and 520.80 ± 28.48 nm respectively at the same ratio. By contrast, AuNCs-Lf-PEI displayed the smallest complex size at a conjugate:DNA weight ratio of 40:1, with an average size of 144.30 ± 6.27 nm. These results demonstrated the AuNCs conjugates ability to condense the DNA into small complexes with sizes suitable for gene delivery.

Zeta potential experiments showed that the AuNCs complexes were bearing a slightly negative surface charge at a conjugate:DNA weight ratio of 0.5:1, indicating that the negatively charged DNA was not fully complexed with AuNCs conjugates at this ratio. The zeta potential then increased as the weight ratios of the complexes increased, to finally reach the maximum positive charges of 19.90 ± 0.45, 26.70 ± 0.37 and 28.70 ± 0.38 mV for AuNCs-Lf, AuNCs-Lf-PEG and AuNCs-Lf-PEI respectively, at a conjugate:DNA weight ratio of 40:1 (Figure 6B). These results were in good agreement with gel retardation findings.

Transfection

AuNCs-Lf, AuNCs-Lf-PEG and AuNCs-Lf-PEI complexed to DNA were found to increase gene expression at optimal AuNCs conjugate:DNA weight ratios, compared with PEI and DOTAP complexes on PC-3 cells (Figure 7).

Higher gene expression in comparison with PEI complex was observed following treatment with AuNCs-Lf complex at conjugate:DNA ratios of 0.5:1, 1:1, 10:1, 20:1, after treatment with AuNCs-Lf-PEG complex at ratios of 0.5:1, 5:1, 10:1 and 40:1, and at ratios 0.5:1, 1:1, 20:1 and 40:1 as a result of treatment with AuNCs-Lf-PEI complex.

The 3 complexes also led to higher gene expression than DOTAP complex at the ratio of 0.5:1, and at a ratio of 40:1 for AuNCs-Lf-PEI complex.

The highest transfection level was observed following treatment with AuNCs-Lf-PEI complex at a ratio of 40:1 (2.49 ± 0.10 mU/mL). It was 2.1-fold higher than when treated with DNA (1.16 ± 0.01 mU/mL), 1.7-fold higher than with PEI complex (1.46 ± 0.05 mU/mL) and 1.4-fold higher than following treatment with DOTAP complex (1.68 ± 0.09 mU/mL).

AuNCs-Lf-PEG complex led to its highest gene expression level at a conjugate:DNA weight ratio of 0.5:1 (2.43 ± 0.21 mU/mL). This was 2.1-, 1.6- and 1.4-fold higher than that obtained with DNA, PEI and DOTAP, respectively.

Similarly to AuNCs-Lf-PEG complex, AuNCs-Lf complex resulted in its highest gene expression at

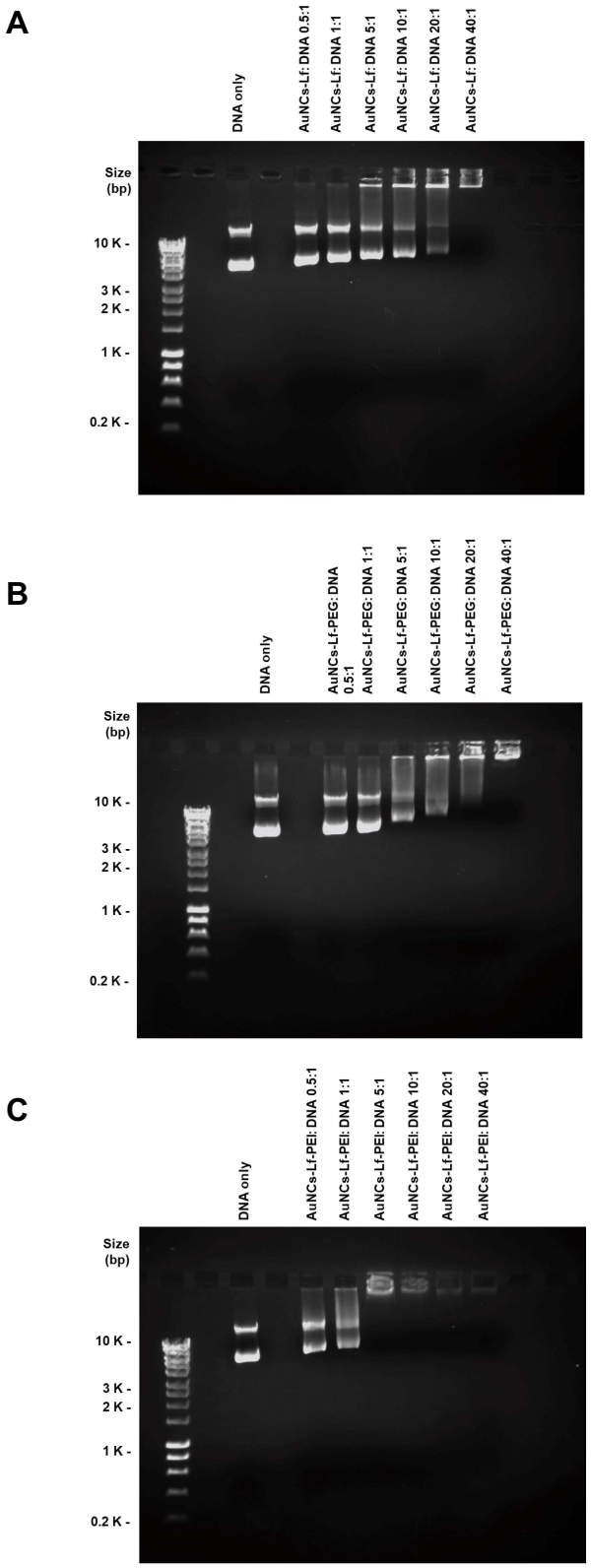

Figure 5 Gel retardation assays of AuNCs-Lf complex (**A**), AuNCs-Lf-PEG complex (**B**) and AuNCs-Lf-PEI complex (**C**) at various conjugate:DNA weight ratios (0.5:1, 1:1, 5:1, 10:1, 20:1, 40:1) (control: DNA solution).

a conjugate:DNA weight ratio of 0.5:1 (2.22 ± 0.24 mU/mL).

The conjugation of PEI to AuNCs-Lf at its optimal conjugate:DNA ratio of 40:1 led to an increased gene transfection (by 1.5-fold) in comparison with unmodified AuNCs-Lf, unlike what observed following conjugation of PEG to AuNCs-Lf, which resulted in similar transfection level. Based on these findings, with consideration of DNA condensation results, the conjugate:DNA ratios of 40:1 and 0.5:1 were selected for cellular uptake experiments.

Cellular Uptake

Quantitative Analysis

The treatment of PC-3 cells with AuNCs-Lf-PEI complexed with fluorescein-labeled DNA at a weight ratio of 40:1 resulted in the highest cellular fluorescence (1726.17 ± 49.71 arbitrary units (a.u.)), which was 2.3-fold and 6.9-fold higher than that observed with AuNCs-Lf and AuNCs-Lf-PEG complexes (725.17 ± 33.93 and 247.50 ± 3.53 a.u. respectively) at the same ratio (Figure 8). It was similar to that observed with PEI complex (1803.5 ± 25.42 a.u.) and 8.6-fold higher than that observed after treatment with DNA solution (199.50 ± 1.31 a.u.). There was no significant difference in DNA cellular uptake following treatment with AuNCs-Lf, AuNCs-Lf-PEG and AuNCs-Lf-PEI complexes at a ratio of 0.5:1.

In addition, the treatment of cells with naked DNA resulted in a weak DNA uptake, indicating the failure of DNA to be taken up by prostate cancer cells without the assistance of a carrier.

Qualitative Analysis

The cellular uptake of fluorescein-labeled DNA complexed with AuNCs-Lf-PEI by PC-3 cells was qualitatively confirmed using confocal microscopy (Figure 9). Fluorescein-labeled DNA was disseminated in the cytoplasm after treatment with AuNCs-Lf-PEI complex. No co-localization of DNA in the nuclei was visible after 24 h incubation. By contrast, the cells treated with DNA solution did not show any fluorescein-derived fluorescence.

Cell Viability

The treatment of PC-3 cells with AuNCs-Lf, AuNCs-Lf-PEG and AuNCs-Lf-PEI resulted in a cell viability higher than 70% at all the tested concentrations

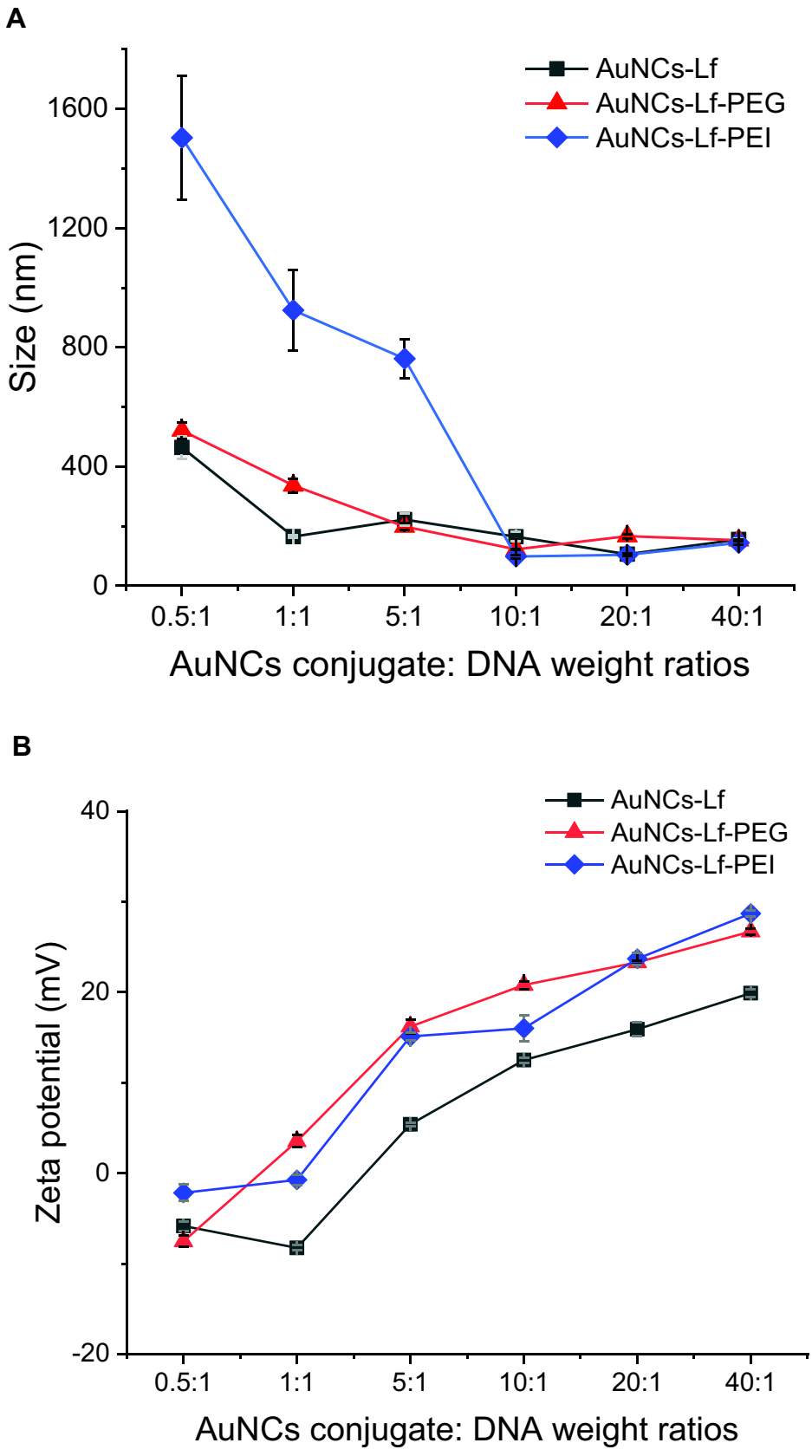

Figure 6 Size (**A**) and zeta potential (**B**) of gold conjugates complexed to DNA at various AuNCs conjugate:DNA weight ratios. Results are expressed as mean ± SEM (n=9).

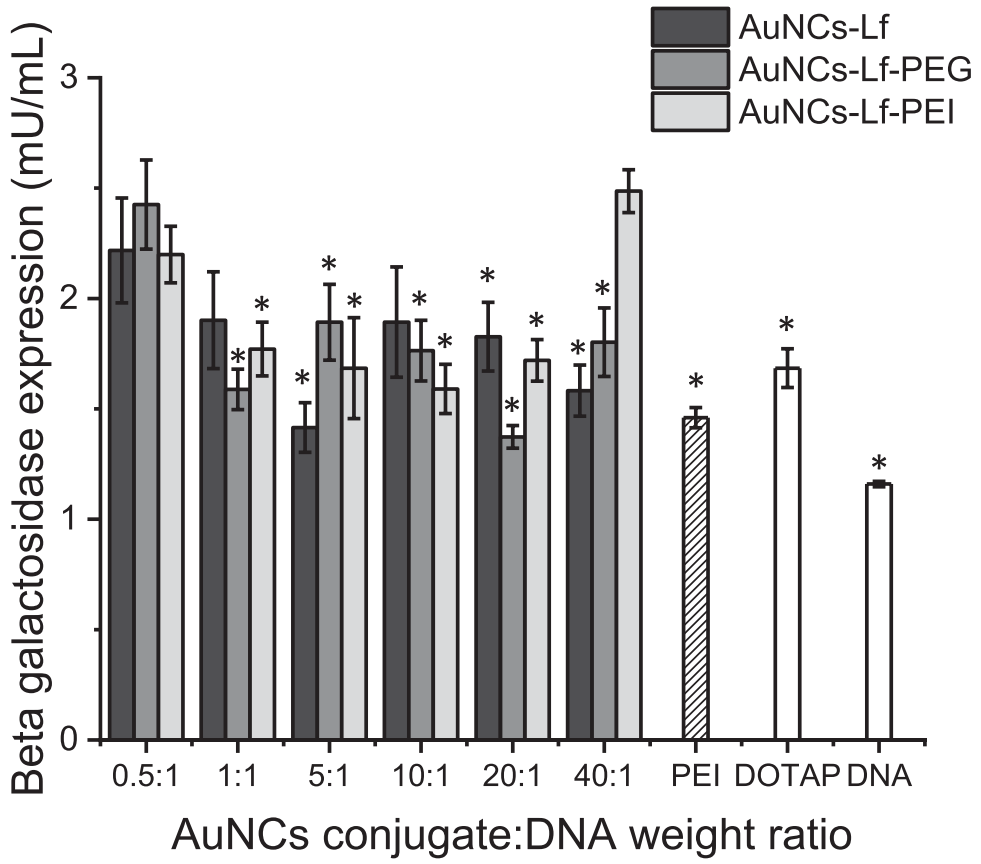

Figure 7 Transfection efficacy of AuNCs-Lf, AuNCs-Lf-PEG and AuNCs-Lf-PEI complexes at various conjugates: DNA weight ratios in PC-3 cells. Results are expressed as the mean ± SEM of three replicates (n=15). *$P < 0.05$ versus the highest transfection ratio.

(Figure 10). At the maximum treatment concentration (200 µg/mL), the cell viability was higher following treatment with AuNCs-Lf-PEG and AuNCs-Lf-PEI (83.39 ± 1.10% and 79.27 ± 1.63% respectively) than with AuNCs-Lf (73.12 ± 1.80%). This increase was attributed to the conjugation of PEG and PEI onto the AuNCs-Lf. These results therefore suggest that AuNCs conjugates are safe towards PC-3 cancer cells at the tested concentrations.

Discussion

The possibility of using gold nanocages as gene delivery systems for cancer treatment has previously been reported in conjunction with photothermal therapy and chemotherapeutics, but has never been assessed in isolation and without external stimulations so far. To explore this possibility, we hypothesize that the conjugation of cancer-targeting lactoferrin, PEG or PEI to gold nanocages complexed to plasmid DNA would lead to enhanced gene expression efficacy in PC-3 prostate cancer cells.

In this study, gold nanocages have been successfully produced through the galvanic replacement reaction between Ag nanocubes and chloroauric acid aqueous solution.[22] The production of a large batch of gold nanocages allowed the elimination of batch-to-batch variations that could have a detrimental impact on the surface conjugation of the gold nanocages, their characterization and in vitro experiments results.[26]

The conjugation of Lf, PEG and PEI was confirmed by using CD and FTIR spectroscopy (in the case of Lf conjugation) and UV-Vis spectrometry analysis (for demonstrating Lf, PEG and PEI grafting). The surface Plasmon resonance of AuNCs-Lf-PEI was 813 nm, following the conjugation of PEI to AuNCs-Lf. This red-shifted resonance compared with that of unmodified AuNCs was attributed to the change of refractive index on the surface of the AuNCs, demonstrating the conjugation of PEI to the surface of AuNCs. This point of absorption would be particularly suitable for further promotion of gene delivery using near-infrared irradiation, as reported by other

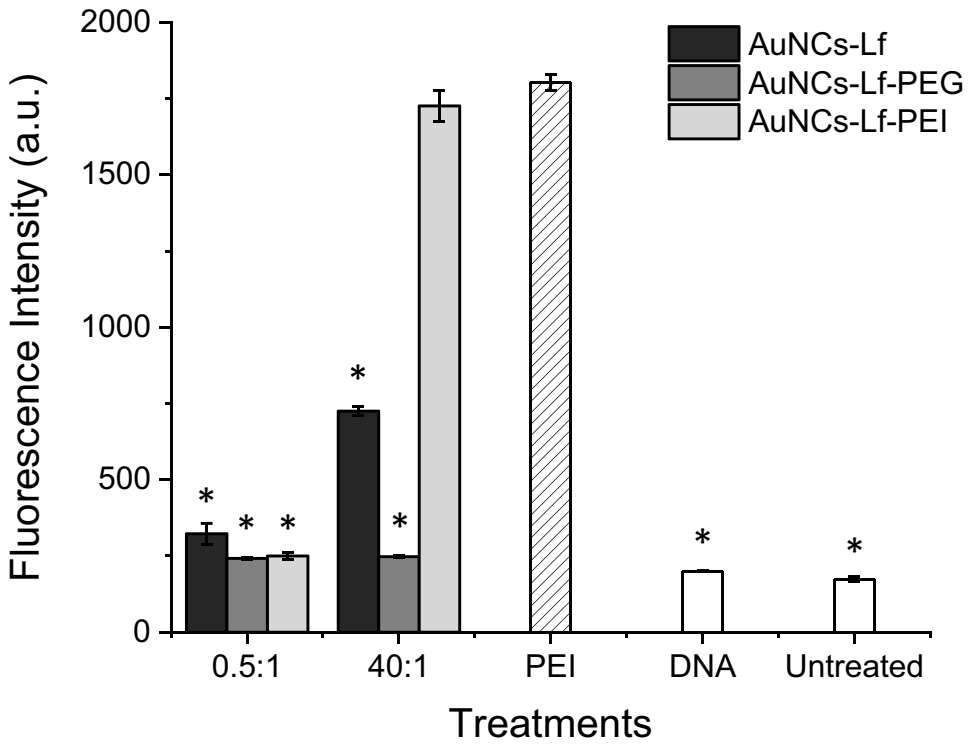

Figure 8 Quantification of the cellular uptake of fluorescein-labeled DNA complexed with AuNCs-Lf, AuNCs-Lf-PEG and AuNCs-Lf-PEI or as a solution, after 24-h incubation with PC-3 cells, using flow cytometry (n = 6). *$P < 0.05$ when compared with PEI-DNA.

groups.[27] All synthesized gold conjugates in this study exhibited UV-Vis spectra peaks in the near-infrared region (700–900 nm), making them appropriate platforms for imaging and photothermal applications.

Crucially, AuNCs-Lf, AuNCs-Lf-PEG and AuNCs-Lf-PEI conjugates were all bearing a positive charge, unlike the unmodified AuNCs, which is of the utmost importance for permitting the complexation of DNA. The AuNCs conjugates were all able to complex the negatively charged DNA through electrostatic interactions, at conjugate:DNA weight ratios of 5:1 and above to ensure efficient DNA condensation. The AuNCs conjugate complexes at these weight ratios displayed suitable size diameter to allow them to penetrate into the cancer cells, as the cut-off size for extravasation was found to be 400 nm for most tumors.[28]

In addition, the conjugation of AuNCs-Lf with PEG and PEI enhanced the DNA complexation efficiency, as AuNCs-Lf-PEG and AuNCs-Lf-PEI conjugates displayed higher positive charges compared to unmodified AuNCs-Lf, whose positive charges were mostly due to the presence of positively charged amino acids within Lf. AuNCs-Lf conjugates therefore have the required physicochemical properties for being efficient gene delivery systems. It is worth noting that DNA condensation efficiency of AuNCs-Lf conjugates could not be assessed using PicoGreen® assay, due to the fluorescence quenching properties of gold nanoparticles and the blue color of the AuNCs samples that interfered with fluorescence intensity measurements and thereby might have led to false-positive results.[29]

The treatment of PC-3 cells with AuNCs-Lf resulted in enhanced transfection at some conjugates: DNA ratios compared to the positive controls PEI and DOTAP. This result was in line with previous publications that reported that the conjugation of Lf to delivery systems significantly improved the gene expression in various cancer cell lines. For instance, Lim et al demonstrated that the conjugation of Lf to generation 3-diaminobutyric polypropylenimine dendrimer (DAB) resulted in a 1.4-fold higher gene expression compared with unconjugated DAB on A431 and B16F10 cells.[13] Similarly, Altwaijry et al reported that treatment of PC-3 cells with DAB-Lf dendriplex led to 2-fold higher gene expression compared to unmodified DAB.[14] In the present study, gene expression following treatment with AuNCs-Lf complex was 1.52- and 1.32-fold higher than that obtained with PEI and DOTAP, respectively. Furthermore, the conjugation of AuNCs-Lf

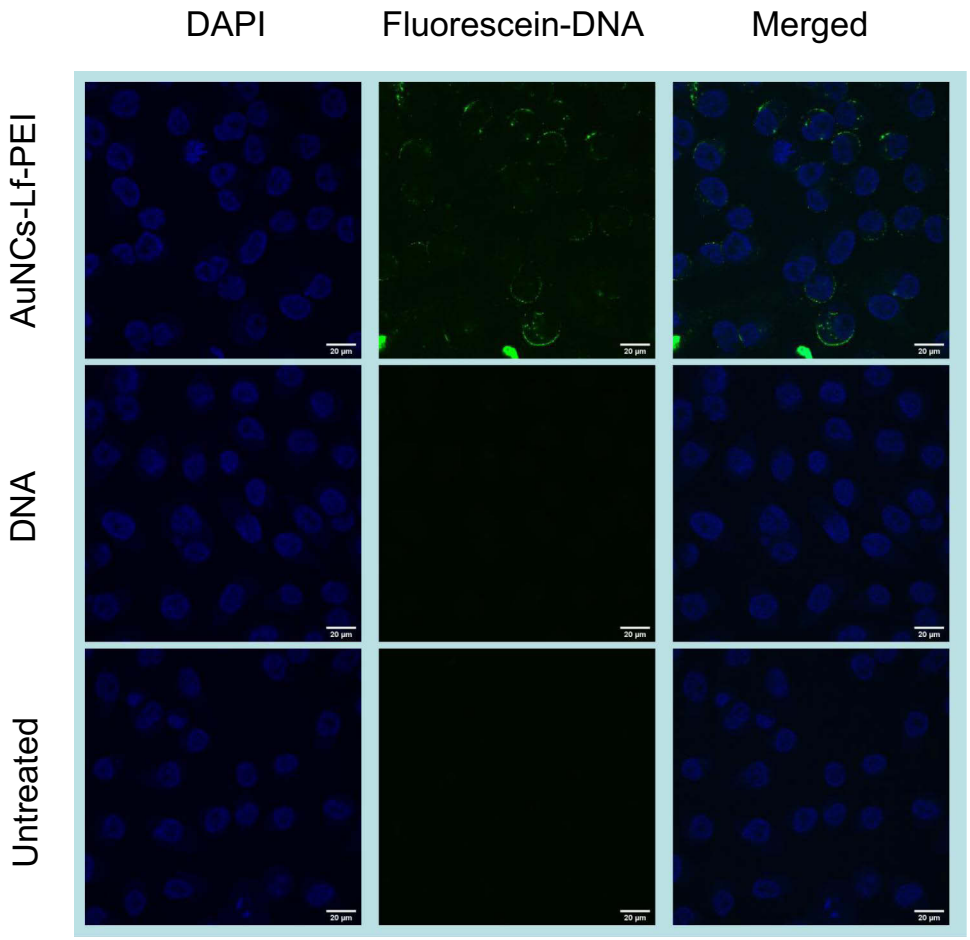

Figure 9 Confocal microscopy images of the cellular uptake of fluorescein-labeled DNA (2.5 μg per well), either complexed with AuNCs-Lf-PEI at a weight ratio of 40:1 or in solution after 24-h incubation with PC-3 cells (control: untreated cells). Blue: nuclei stained with DAPI (excitation: 405 nm laser line; bandwidth: 415–491 nm), green: fluorescein-labeled DNA (excitation: 453 nm laser line; bandwidth: 550–620 nm) (bar: 20 μm).

with PEI and PEG led to an enhanced gene transfection in comparison with unmodified AuNCs-Lf. Gene expression following treatment with AuNCs-Lf-PEI and AuNCs-Lf-PEG complexes at AuNCs conjugate:DNA ratios of 40:1 for AuNCs-Lf-PEI and 5:1 for AuNCs-Lf-PEG was respectively 1.58-fold and 1.33-fold higher than that obtained from AuNCs-Lf complex. The grafting of PEG onto AuNCs-Lf, which increased the transfection efficiency by 1.45- and 1.66-fold compared with DOTAP and PEI, has previously been shown to improve gene transfection of various delivery systems. For example, Somani et al reported that PEGylated dendrimers showed significantly higher transfection levels than non-PEGylated dendrimers in B16F10-Luc, A431, T98G, DU145 and PC-3-Luc cancer cell lines.[20] Additionally, Luan et al demonstrated that the PEGylation of gold nanoparticles led to a significantly increased gene silencing in PC-3 cells compared to Lipofectamine® 2000, a lipid-based transfection reagent used as a positive control.[30] It has recently been reported that the PEGylation of gold nanoparticles resulted in an increase in transfection efficiency and cellular uptake by more than 45%, with low cytotoxicity, compared with non-PEGylated nanoparticles, therefore making PEGylated gold nanoparticles suitable vehicles for DNA delivery.[31] The transfection efficiency following the treatment with AuNCs-Lf-PEI complex was 1.71-fold higher than PEI and 1.48-fold higher than DOTAP. This result was in accordance with previous studies that demonstrated that the conjugation of gold nanoparticles with PEI improves the transfection efficiency.[32,33] The increase of β-galactosidase expression induced by AuNCs-Lf-PEG and AuNCs-Lf-PEI conjugates compared to unmodified AuNCs-Lf most likely resulted from the higher zeta potential of their DNA complexes, as a result of the strong correlation between cellular uptake and positive charge density of complexes.[34] In

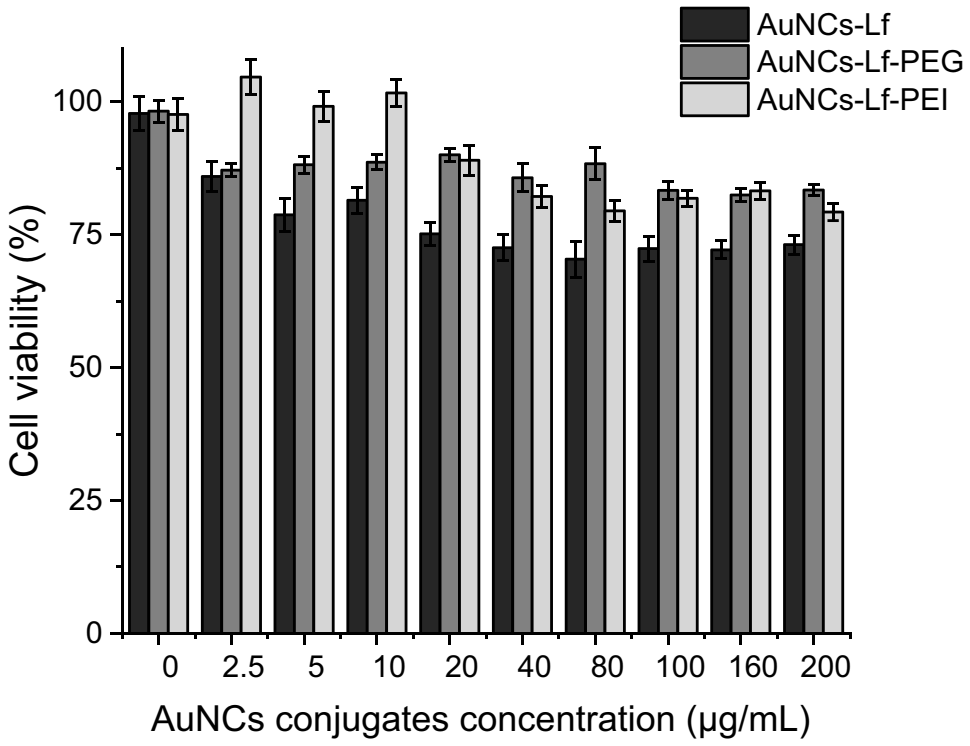

Figure 10 Cell viability of PC-3 prostate cancer cell treated with AuNCs-Lf, AuNCs-Lf-PEG and AuNCs-Lf-PEI at various concentrations (n=15).

addition to that, the highest transfection efficacy of AuNCs-Lf-PEI was also due to the proton sponge effect of PEI, which highly facilitates the endosomal escape.[24,35]

The cellular uptake of DNA complexed to AuNCs-Lf-PEI was significantly enhanced in comparison to that obtained with unmodified AuNCs-Lf, due to the presence of PEI which mediated proton sponge effect, leading to an improved endosomal escape of DNA. On the other hand, AuNCs-Lf-PEG led to a lower level of DNA uptake after 24 h incubation in comparison with AuNCs-Lf, leading to the hypothesis that the DNA uptake following this treatment occurred at a later time, owing to the PEG effect in reducing cellular uptake that has been previously reported.[36]

Future work should assess the interactions of AuNCs-Lf conjugates with the protein corona for potential in vivo applications. When exposed to biological fluids, nanoparticles tend to interact with biomolecules, leading to the formation of a complex layer of proteins, the protein corona. The presence of this protein corona on the surface of nanoparticles has previously been shown to impact the cellular internalization of the delivery systems and the release of the entrapped drugs, modifying the biological response in vivo.[37,38] It is hoped that the surface modification of AuNCs with Lf, PEG and PEI could minimize protein adsorption and alter the corona composition, as a study by Assali et al[39] previously reported that functionalized gold nanoplatforms displayed less interactions with proteins and adsorbed less opsonins than their unmodified counterparts.

Conclusion

We have demonstrated for the first time that novel gold nanocages conjugated to lactoferrin, PEI and PEG and complexed to plasmid DNA led to an increase in gene expression in PC-3 prostate cancer cells. Cell viability data demonstrated the low toxicity of these gold conjugates, with cell viability higher than 70% at all the tested concentrations. Among the conjugates, gold nanocages conjugated to lactoferrin and PEI led to the highest transfection level on PC-3 cells, compared to DOTAP and PEI. This was probably due to the significant increase in cellular uptake of DNA in PC-3 prostate cancer cell line following treatment with this complex, compared with what that observed in cells treated with DNA solution. To our knowledge, this is the first time lactoferrin-bearing gold nanocages have been used to target prostate cancer cells, leading to enhanced DNA uptake and gene expression in PC-3 prostate cancer cells without external stimulation. Lactoferrin-bearing gold

nanocages conjugates are therefore promising gene nanocarriers to prostate cancer cells and will be further investigated, alone or in combination with other cancer therapy.

Abbreviations

AgCl, silver chloride; ANOVA, one-way analysis of variance; ATR, attenuated total reflectance; AuNCs, gold nanocages; AuNCs-Lf, lactoferrin-bearing AuNCs; AuNCs-Lf-PEG, PEG-conjugated, lactoferrin-bearing gold nanocages; AuNCs-Lf-PEI, PEI-conjugated, lactoferrin-bearing gold nanocages; CD, circular dichroism; CF_3COOAg, silver trifluoroacetate; DAPI, 4′,6-diamidino-2-phenylindole; DEG, diethylene glycol; DI, deionized water; DNA, deoxyribonucleic acid; DOTAP, N-[1-(2,3-Dioleoyloxy) propyl]-N,N, N-trimethylammonium methylsulfate; FBS, fetal bovine serum; FTIR, Fourier-transform infrared; $HAuCl_4$, chloroauric acid; HCl, aqueous hydrochloric acid solution; HS-PEG3.5K-NH_2, thiol PEG amine; ICP-MS, inductively coupled plasma mass spectrometry; Lf, lactoferrin; MEM, Modified Eagle Medium; MWCO, molecular weight cut-off; NaCl, sodium chloride; NaSH, sodium hydrosulfide hydrate; PEG, polyethylene glycol; PEI, polyethylenimine; PLB, passive lysis buffer; PVP, polyvinyl pyrrolidone; RNA, ribonucleic acid; S.E.M., standard error of the mean; TBE, Tris-Borate-EDTA; TEM, transmission electron microscopy.

Acknowledgments

This work was financially supported by a PhD studentship from the Saudi Arabian Cultural Bureau in the UK and Umm Al-Qura University (Kingdom of Saudi Arabia) to J.A. S.S. is funded by a research grant from The Dunhill Medical Trust [grant number R463/0216]. P.L. is funded by a research grant from the Worldwide Cancer Research [grant number 16–1303]. The authors would like to acknowledge Mr Alexander Clunie for his help with the ICP-MS experiments and CMAC National Facility, housed within the University of Strathclyde's Technology and Innovation Centre, and funded with a UK Research Partnership Institute Fund (UKRPIF) for the access to the CD instrument.

Disclosure

The authors report no conflicts of interest in this work.

References

1. Chen J, Wang D, Xi J, et al. Immuno gold nanocages with tailored optical properties for targeted photothermal destruction of cancer cells. *Nano Lett*. 2007;7:1318–1322. doi:10.1021/nl070345g
2. Sun T, Zhang YS, Pang B, et al. Engineered nanoparticles for drug delivery in cancer therapy. *Angew Chem Int Ed Engl*. 2014;53:12320–12364. doi:10.1002/anie.201403036
3. Beik J, Khateri M, Khosravi Z, et al. Gold nanoparticles in combinatorial cancer therapy strategies. *Coord Chem Rev*. 2019;387:299–324. doi:10.1016/j.ccr.2019.02.025
4. McIntosh CM, Esposito EA, Boal AK, et al. Inhibition of DNA transcription using cationic mixed monolayer protected gold clusters. *J Am Chem Soc*. 2001;123(31):7626–7629. doi:10.1021/ja015556g
5. Oishi M, Nakaogami J, Ishii T, et al. Smart PEGylated gold nanoparticles for the cytoplasmic delivery of siRNA to induce enhanced gene silencing. *Chem Lett*. 2006;35(9):1046–1047. doi:10.1246/cl.2006.1046
6. Rosi NL, Giljohann DA, Thaxton CS, et al. Oligonucleotide-modified gold nanoparticles for intracellular gene regulation. *Science*. 2006;312:1027–1030. doi:10.1126/science.1125559
7. Fitzgerald KA, Rahme K, Guo J, et al. Anisamide-targeted gold nanoparticles for siRNA delivery in prostate cancer–synthesis, physicochemical characterisation and *invitro* evaluation. *J Mater Chem B*. 2016;4(13):2242–2252. doi:10.1039/C6TB00082G
8. Skrabalak SE, Chen J, Sun Y, et al. Gold nanocages: synthesis, properties, and applications. *Acc Chem Res*. 2008;41:1587–1595. doi:10.1021/ar800018v
9. Chen J, Glaus C, Laforest R, et al. Gold nanocages as photothermal transducers for cancer treatment. *Small*. 2010;6:811–817. doi:10.1002/smll.200902216
10. Xia X, Xia Y. Gold nanocages as multifunctional materials for nanomedicine. *Front Phys*. 2014;9:378–384. doi:10.1007/s11467-013-0318-8
11. Li W, Cai X, Kim C, et al. Gold nanocages covered with thermally-responsive polymers for controlled release by high-intensity focused ultrasound. *Nanoscale*. 2011;3(4):1724–1730. doi:10.1039/c0nr00932f
12. Yavuz MS, Cheng Y, Chen J, et al. Gold nanocages covered by smart polymers for controlled release with near-infrared light. *Nat Mater*. 2009;8:935–939. doi:10.1038/nmat2564
13. Lim LY, Koh PY, Somani S, et al. Tumor regression following intravenous administration of lactoferrin-and lactoferricin-bearing dendriplexes. *Nanomedicine*. 2015;11:1445–1454. doi:10.1016/j.nano.2015.04.006
14. Altwaijry N, Somani S, Parkinson JA, et al. Regression of prostate tumors after intravenous administration of lactoferrin-bearing polypropylenimine dendriplexes encoding TNF-α, TRAIL, and interleukin-12. *Drug Deliv*. 2018;25:679–689. doi:10.1080/10717544.2018.1440666
15. Altwaijry N, Somani S, Dufès C. Targeted non-viral gene therapy in prostate cancer. *Int J Nanomedicine*. 2018;13:5753–5767. doi:10.2147/IJN.S139080
16. Sullivan MO, Green J, Przybycien T. Development of a novel gene delivery scaffold utilizing colloidal gold–polyethylenimine conjugates for DNA condensation. *Gene Ther*. 2003;10:1882–1890. doi:10.1038/sj.gt.3302083
17. Hu C, Peng Q, Chen F, et al. Low molecular weight polyethylenimine conjugated gold nanoparticles as efficient gene vectors. *Bioconjug Chem*. 2010;21(5):836–843. doi:10.1021/bc900374d
18. Kong WH, Sung DK, Shim YH, et al. Efficient intracellular siRNA delivery strategy through rapid and simple two steps mixing involving noncovalent post-PEGylation. *J Control Release*. 2009;138:141–147. doi:10.1016/j.jconrel.2009.04.034

19. Ping Y, Liu C, Zhang Z, et al. Chitosan-graft-(PEI-β-cyclodextrin) copolymers and their supramolecular PEGylation for DNA and siRNA delivery. *Biomaterials*. 2011;32(32):8328–8341. doi:10.1016/j.biomaterials.2011.07.038
20. Somani S, Laskar P, Altwaijry N, et al. PEGylation of polypropylenimine dendrimers: effects on cytotoxicity, DNA condensation, gene delivery and expression in cancer cells. *Sci Rep*. 2018;8:1–13. doi:10.1038/s41598-018-27400-6
21. Wang Y, Zheng Y, Huang CZ, et al. Synthesis of Ag nanocubes 18–32 nm in edge length: the effects of polyol on reduction kinetics, size control, and reproducibility. *J Am Chem Soc*. 2013;135:1941–1951. doi:10.1021/ja311503q
22. Skrabalak SE, Au L, Li X, et al. Facile synthesis of Ag nanocubes and Au nanocages. *Nat Protoc*. 2007;2(9):2182–2190. doi:10.1038/nprot.2007.326
23. Johnsen KB, Bak M, Kempen PJ, et al. Antibody affinity and valency impact brain uptake of transferrin receptor-targeted gold nanoparticles. *Theranostics*. 2018;8(12):3416. doi:10.7150/thno.25228
24. Kang HC, Kang H-J, Bae YH. A reducible polycationic gene vector derived from thiolated low molecular weight branched polyethyleneimine linked by 2-iminothiolane. *Biomaterials*. 2011;32(4):1193–1203. doi:10.1016/j.biomaterials.2010.08.079
25. Zinselmeyer BH, Mackay SP, Schätzlein AG, Uchegbu IF. The lower-generation polypropylenimine dendrimers are effective gene-transfer agents. *Pharm Res*. 2002;19:960–967. doi:10.1023/A:1016458104359
26. Avvakumova S, Pandolfi L, Soprano E, et al. Does conjugation strategy matter? Cetuximab-conjugated gold nanocages for targeting triple-negative breast cancer cells. *Nanoscale Adv*. 2019;1:3626–3638. doi:10.1039/C9NA00241C
27. Assali A, Akhavan O, Adeli M, et al. Multifunctional core-shell nanoplatforms (gold@graphene oxide) with mediated NIR thermal therapy to promote miRNA delivery. *Nanomedicine*. 2018;14:1891–1903. doi:10.1016/j.nano.2018.05.016
28. Yuan F, Dellian M, Fukumura D, et al. Vascular permeability in a human tumor xenograft: molecular size dependence and cutoff size. *Cancer Res*. 1995;55:3752–3756.
29. Xia X, Yang M, Oetjen LK, et al. An enzyme-sensitive probe for photoacoustic imaging and fluorescence detection of protease activity. *Nanoscale*. 2011;3:950–953. doi:10.1039/c0nr00874e
30. Luan X, Rahme K, Cong Z, et al. Anisamide-targeted PEGylated gold nanoparticles designed to target prostate cancer mediate: enhanced systemic exposure of siRNA, tumour growth suppression and a synergistic therapeutic response in combination with paclitaxel in mice. *Eur J Pharm Biopharm*. 2019;137:56–67. doi:10.1016/j.ejpb.2019.02.013
31. Zamora-Justo JA, Abrica-González P, Vázquez-Martínez GR, et al. Polyethylene glycol-coated gold nanoparticles as DNA and atorvastatin delivery systems and cytotoxicity evaluation. *J Nanomater*. 2019;2019:. doi:10.1155/2019/5982047
32. Thomas M, Klibanov AM. Conjugation to gold nanoparticles enhances polyethylenimine's transfer of plasmid DNA into mammalian cells. *Proc Natl Acad Sci U S A*. 2003;100:9138–9143. doi:10.1073/pnas.1233634100
33. Sharma A, Tandon A, Tovey JC, et al. Polyethylenimine-conjugated gold nanoparticles: gene transfer potential and low toxicity in the cornea. *Nanomedicine*. 2011;7:505–513. doi:10.1016/j.nano.2011.01.006
34. Futaki S, Ohashi W, Suzuki T, et al. Stearylated arginine-rich peptides: a new class of transfection systems. *Bioconjug Chem*. 2001;12:1005–1011. doi:10.1021/bc015508l
35. Creusat G, Rinaldi AS, Weiss E, et al. Proton sponge trick for pH-sensitive disassembly of polyethylenimine-based siRNA delivery systems. *Bioconjug Chem*. 2010;21:994–1002. doi:10.1021/bc100010k
36. Mishra S, Webster P, Davis ME. PEGylation significantly affects cellular uptake and intracellular trafficking of non-viral gene delivery particles. *Eur J Cell Biol*. 2004;83:97–112. doi:10.1078/0171-9335-00363
37. Monopoli MP, Åberg C, Salvati A, Dawson KA. Biomolecular coronas provide the biological identity of nanosized materials. *Nat Nanotechnol*. 2012;7:779–786. doi:10.1038/nnano.2012.207
38. Nguyen VH, Lee BJ. Protein corona: a new approach for nanomedicine design. *Int J Nanomedicine*. 2017;12:3137–3151. doi:10.2147/IJN.S129300
39. Assali A, Razzazan S, Akhavan O, et al. The bio-interface between functionalized Au NR@ GO nanoplatforms with protein corona and their impact on delivery and release system. *Colloids Surf B Biointerfaces*. 2019;173:891–898. doi:10.1016/j.colsurfb.2018.10.042